Thermoelectric Power of Bismuth Nanocomposites

Joseph P. Heremans, Christopher M. Thrush, Donald T. Morelli, and Ming-Cheng Wu
Delphi Research Labs, Delphi Corporation, Shelby Township, Michigan 48315
(Received 8 February 2002; published 7 May 2002)

Because of the increase in the electronic density of states in low-dimensional systems, semiconductor quantum wires constitute a most promising thermoelectric material. We report here the first experimental observation of a very large enhancement of the thermoelectric power of composites containing bismuth nanowires with diameters of 9 and 15 nm, embedded in porous alumina and porous silica. The temperature dependence of the electrical resistance shows that the samples are semiconductors with energy gaps between 0.17 and 0.4 eV, consistent with the theoretical predictions.

DOI: 10.1103/PhysRevLett.88.216801 PACS numbers: 73.63.Nm

The seminal work of Molina and Rowland [1] in 1974 first suggested that chlorofluorocarbon compounds, principally freon (R-12), the refrigerant of choice in air conditioning systems for the past 50 years, were destroying the protective ozone layer in the stratosphere at an alarming rate. The Montreal Protocol of 1987 has led to the gradual phasing out of these chemicals. Non-chlorine-containing fluorocarbons, such as R-134a, which do not possess the long-term stability of R-12, have received widespread use as refrigerants. It was not realized until quite recently, however, that all fluorocarbons, including both R-12 and R-134a, could contribute to global warming [2]. Thermoelectricity is one alternative climate control technology that does not contain such chemicals and presents many additional advantages including all-solid-state operation without moving parts, electronic capacity control, reversibility to provide both heating and cooling, and high reliability. Thermoelectric heat-to-electrical power converters also have potential uses in thermal energy recovery systems. However, thermoelectric cooling has not enjoyed widespread use because of its low efficiency relative to vapor compression systems. The thermoelectric efficiency (or coefficient of performance for a cooler) depends on the thermoelectric figure of merit, Z, of the material of which the thermoelectric device is comprised. This quantity is a combination of the thermoelectric power or Seebeck coefficient S, the electrical conductivity σ, and the thermal conductivity κ of the material:

$$Z = \frac{S^2\sigma}{\kappa}. \quad (1)$$

Currently, the bulk material with the highest thermoelectric figure of merit at room temperature (300 K) is Bi_2Te_3 with $Z = 0.003\ K^{-1}$, but an improvement by about a factor of 2 is necessary [3] for thermoelectric devices to be competitive with vapor-compression technology.

One approach to increasing Z is to search for physical systems exhibiting an enhanced thermoelectric power. In 1993, Hicks and Dresselhaus [4] pointed out that, due to the quantum-mechanical nature of the motion of electrons through solids, confining such electrons in a structure with a physical dimension below the spatial extent of the electron wave function should result in an enhancement of Z. The main mechanism for the enhancement is due to an increase of the density of states near the Fermi level: As a result, a sufficient density of charge carriers can exist in the solid to maintain the electrical conductivity, but the Fermi energy is small, and this leads to a large S. An enhancement of Z has been reported recently [5] in superlattices, but the authors ascribe that effect to a control of the phonon thermal conductivity at the interfaces. Furthermore, superlattices are more suitable for thin-film applications than for large-scale climate control. Stronger increases in Z are predicted [4,6] in quantum wires because of the additional confinement: The electronic density of states is characterized by the existence of peaks at quantized values of energy. Bismuth is a particularly attractive candidate, because the electronic effective mass is very small along certain crystallographic directions in this semimetal, and therefore the spatial extent of the electron wave functions is large. Furthermore, its lattice thermal conductivity is small, because it is the heaviest nonradioactive element. According to Ref. [6], which constitutes the theoretical basis for the work presented here, Bi nanowires become semiconductors when the diameter is decreased below 50 nm. An enhancement of the figure of merit to a value of $ZT = 6$ (at 77 K) is predicted for wires with 5 nm diameters, doped to 10^{18} electrons per cm^3.

While the theoretical basis for the increase in S and Z has been developed, experimental verification of these effects has been difficult to realize, with this Letter describing the first enhancement in the thermoelectric power ever observed. The first hurdle is the sample synthesis technique. Molten bismuth has been inserted into porous hosts under very high pressures [7], but this technique is limited to wires with diameters greater than 40 to 50 nm, because the necessary pressure increases rapidly with decreasing diameter. Nevertheless, this technique has been used to prepare the first wires on which the metal/semiconductor transition was reported, as evidenced by magnetoresistance data [8]. A new vapor-phase technique was developed by us [9], and, since it does not depend on the surface tension of the bismuth/host material interface, it has been used to prepare wires of diameters down to 7 nm. The temperature

dependence of the electrical resistance of nanowires of diameters in the 200 to 7 nm range, and their magnetoresistance, illustrates the transition very clearly [9]. Until now, the thermoelectric power was measured only on 200 nm wires [10], which are metallic and show no enhancement in S, as expected [6].

In this work, we use as host materials a commercially available silica gel (SiO_2), and a specially prepared porous alumina (Al_2O_3). We introduce Bi in the network of pores that permeates these hosts, and report a large enhancement of the thermoelectric power in these composites. The samples are bulk, macroscopic Bi/SiO_2 or Bi/Al_2O_3 nanocomposites. As control samples, we prepare Zn/SiO_2 and Zn/Al_2O_3 nanocomposites in an identical fashion, and show that they do remain metallic with a very small thermoelectric power.

The first type of host material used for this work is commercially available silica gel, Whatman K5, which has pores on the order of 15 nm. The porous grains, which have diameters of about 10 μm, are bonded by an organic binder, which pyrolyzes during the introduction of Bi. The second type of host material is prepared from a slurry of Al_2O_3, comprising 66 wt % of θ-Al_2O_3 grains, 31 wt % of milled α-Al_2O_3 grains, and 3 wt % aluminum nitrate $[Al(NO_3)_3 9H_2O]$ binder, based on the total weight of solids. The θ-Al_2O_3 grains have a pore size distribution of an approximate Gaussian shape centered at 9 nm with full width at half maximum of 7 nm, as measured by a pulse equilibrium adsorption technique based on the Kelvin equation [11]. The nonporous α-Al_2O_3 grains are necessary for the mechanical integrity of the samples after preparation. Because they are electrically insulating, their presence greatly increases the resistance of the sample, thus decreasing Z. The slurry was dried and then calcined overnight at 270 °C in air; this drives out the nitrate and fuses the grains to each other with Al_2O_3.

To introduce the Bi, 0.5 mm thick freestanding plates of silica and alumina host material were put on top of a crucible in a cryopumped vacuum chamber, in the manner described previously [9]. After a brief outgassing period (using a heater located on top of the sample, and not used in Ref. [9]) in vacuum near 640 $\pm$ 10 °C, the samples were held at 590 $\pm$ 10 °C in the presence of Bi vapor for 4 min, and then cooled slowly [9]. The two samples of each Bi composite on which transport data are reported below were prepared in two separate runs. For comparison, we also prepared samples of SiO_2 and Al_2O_3 with the pores filled with Zn; the preparation technique was identical as for the Bi nanocomposites, except for the growth temperature, which started near 480 °C. X-ray diffraction measurements were taken on samples that were lapped 0.2 mm deep, so as to avoid peaks generated by metal particles that may remain on the surfaces after the exposure to the vapor. The spectra on the Bi nanocomposites show the presence of rhombohedral Bi peaks; similarly, x-ray diffraction data on the Zn/Al_2O_3 samples have peaks corresponding to hexagonal Zn. A cursory linewidth analysis using the Scherer formula gives Bi crystallite sizes for the Bi/SiO_2 composites of about 20 to 50 nm, and for the Bi/Al_2O_3 samples varying from 15 to 50 nm. The discrepancy between these numbers and those obtained by the adsorption technique probably reflects the fact that the wires are cylindrical, and are much longer than wide. Scanning electron microscopy (SEM) was also used to study the structure of the Bi composites. An image of two porous SiO_2 grains, with Bi nanowires extruded out of the one in the forefront (possibly because Bi expands on solidification), is shown in Fig. 1. This study did not reveal traces of Bi coating the outer surfaces of the SiO_2 or Al_2O_3 grains; the metals are absorbed inside the porous grains. Contact between the grains appears to occur via nanowires that extend beyond the grain perimeter. Other SEM images, not shown, show wires of diameters at the resolution of our microscope, about 15 nm.

Two samples of the 15 nm Bi/SiO_2 composite and two samples of the 9 nm Bi/Al_2O_3 composite were mounted for thermoelectric power and electrical resistance measurements. We used two different measurement techniques on the 15 nm Bi/SiO_2 composites, a two-wire technique [10] and a conventional four-wire technique, using two absolute copper/constantan thermocouples to measure the temperature gradient [12]. The latter technique requires no electrical isolation between the thermocouples and the sample, and the copper leg of each thermocouple can be used to probe the electrical potential. The samples were typically 2 mm long along the direction of the thermal gradient, with a cross section of 1×0.5 mm^2; the distance between the thermocouple legs was on the order of 1 mm. The contacts to the samples are made using silver

FIG. 1. Scanning electron micrograph showing two grains of Bi/SiO_2 nanocomposite. Bi nanowires extend beyond the grain perimeter, and assure electrical contacts between the grains. The wire diameters cannot be estimated from this image, because the nanowires are subject to mechanical vibrations, and very low beam voltages and currents were used to avoid melting the Bi.

epoxy, or Wood's alloy. Only the four-contact technique was used on the Bi/Al_2O_3 and Zn/Al_2O_3 composites. All samples were mounted in a liquid helium variable temperature cryostat, and steady-state dc measurement techniques were used. The sample resistance was measured using positive and negative currents, and the voltage was measured using a Keithley 617 electrometer, with a 10^{14} Ω input impedance. The thermoelectric power was measured by applying a temperature gradient using the resistive heater, waiting for it to stabilize, and measuring the temperature and voltage gradients. Again, the electrometer was used to measure the voltage, and, insofar as the sample resistance was low enough to permit it, the measurements were repeated using a Keithley 182 nanovoltmeter, which has an input impedance of 10^{10} Ω.

The temperature dependence of the resistance of the samples, normalized to the resistance at 300 K, is shown in Fig. 2. As the filling fraction of the host alumina and silica materials is unknown, we cannot deduce an intrinsic resistivity. The two Bi/Al_2O_3 samples had room temperature resistances of $R(300\ \mathrm{K}) = 1.2$ and 6.0 GΩ; the two Bi/SiO_2 samples had $R(300\ \mathrm{K}) = 3$ and 16 MΩ. Generally, the sample resistance shows an activated behavior at high temperature, following an equation that reflects the temperature dependence of the intrinsic electron density in a semiconductor [13]:

$$R(T) = R_0 \exp(E_g/2k_BT), \qquad (2)$$

with E_g the energy gap. The solid lines in Fig. 2 are fits of the high-temperature data to Eq. (2) for the four samples studied. The value of E_g for the 15 nm Bi/SiO_2 composites is on the order of 0.18 eV, and 0.29 and 0.39 eV for the 9 nm Bi/Al_2O_3 composites. Assuming that the samples consist of mainly trigonal quantum wires at an average temperature of 250 K, we calculate from Ref. [6] $E_g \approx 0.23$ eV for 15 nm Bi wires and $E_g \approx 0.47$ eV for 9 nm Bi wires. For wires along the bisectrix direction, the numbers are $E_g \approx 0.07$ eV (15 nm) and $E_g \approx 0.2$ eV (9 nm). Given the polycrystalline nature of the sample, we expect the experimental data to fall in between, and the agreement is quite reasonable.

Figure 3 shows the temperature dependence of the resistance of the Zn nanocomposite samples, normalized to the resistance at 300 K. The latter is $R(300\ \mathrm{K}) = 1.7$ kΩ for the Zn/Al_2O_3 sample, and $R(300\ \mathrm{K}) = 0.48$ Ω for the Zn/SiO_2 sample. The resistance of the 15 nm Zn/SiO_2 nanocomposite follows a T^1 law shown as a full line, characteristic of a metal. The resistance of the 9 nm diameter Zn/Al_2O_3 nanocomposite is also fit by a full line showing the sum of a T^1 law, which dominates at high temperature, and a $T^{-1/2}$ law characteristic of localization [14]. We see no evidence of exponential behavior of the resistance in the case of the Zn wires. We take this to indicate that the behavior reported here for the Bi nanocomposites is due to their semiconducting nature.

The absolute value of the thermoelectric power of the Bi nanocomposites studied is shown in Fig. 4, along with the thermoelectric power of bulk Bi and 200 nm Bi wires in anodic alumina [10]. The temperature dependence of the thermoelectric power in the latter two sets of data is metallic, while the nanocomposites are semiconductors, as shown in Fig. 2. A substantial

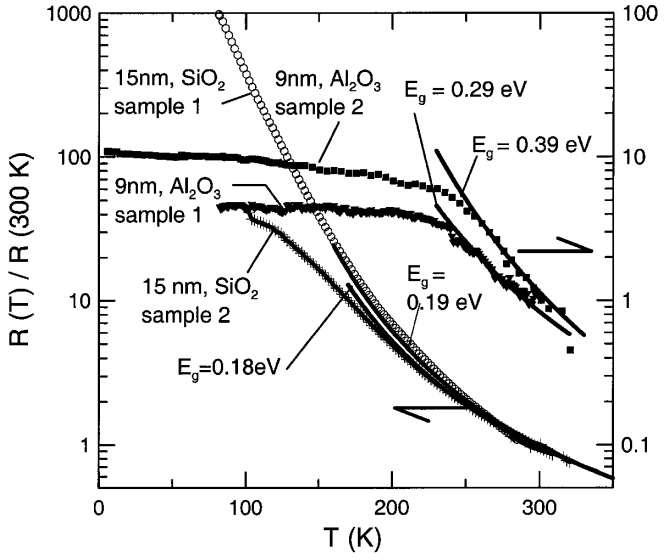

FIG. 2. Temperature dependence of the resistance of the samples of bismuth/silica and of bismuth/alumina nanocomposites, normalized to the resistance at 300 K. The experimental results are shown as data points; the full lines represent fits to Eq. (2), with energy gap values indicated. The left ordinate applies to the two Bi/SiO_2 composites, and the right ordinate to the Bi/Al_2O_3 nanocomposites.

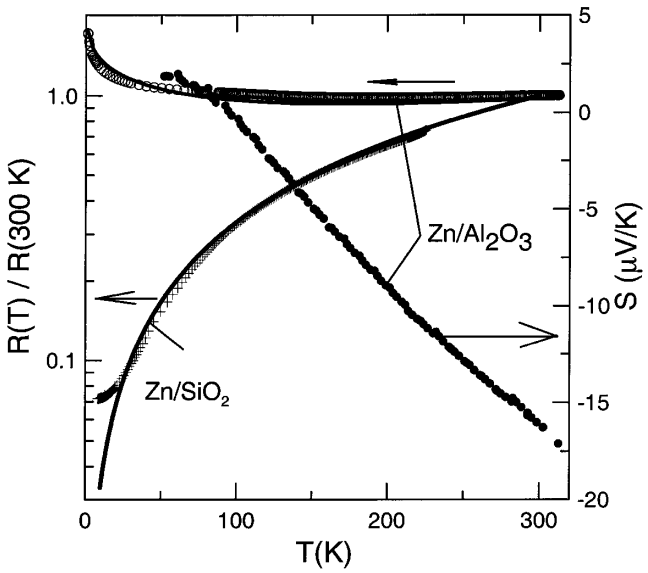

FIG. 3. Temperature dependence of the resistance of the Zn nanocomposites, normalized to the resistance at 300 K (left ordinate). The thermoelectric power (right ordinate) of the Zn/Al_2O_3 nanocomposites is also shown, as full circles. The data are given as points; the full lines are fits to a T^1 law for Zn/SiO_2, and a combined T^1 and $T^{-1/2}$ law for Zn/Al_2O_3.

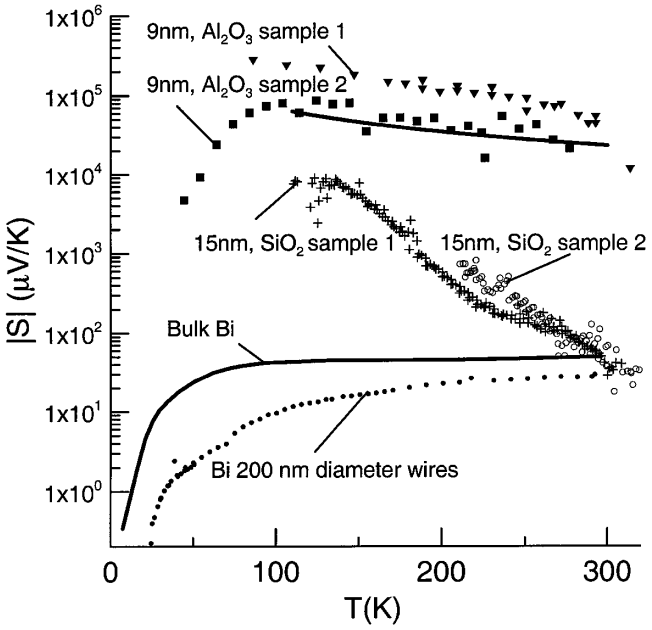

FIG. 4. Absolute value of the thermoelectric power of the two 15 nm bismuth/silica samples, and the two 9 nm bismuth/alumina nanocomposite samples, given as a function of temperature. The thermoelectric power of bulk Bi and that of 200 nm bismuth/anodic alumina reported in the literature [10] are also shown. The thermoelectric power of bulk Bi, the 200 nm wires, and of the Bi/SiO_2 composites is negative; that of the Bi/Al_2O_3 samples is positive. The full line on top is a fit to a T^1 law.

increase in the magnitude of the thermoelectric power is observed in the nanocomposite samples, compared to that of the bulk samples. This behavior is consistent with the picture presented in the previous paragraph of a sharply peaked density of states, with the Fermi energy located near the energy of the peak. A consequence of this quantization, a strongly enhanced thermoelectric power, is demonstrated experimentally for the first time here; this validates the approach of using nanostructures to enhance the thermoelectric figure of merit. The thermoelectric power of the Bi/Al_2O_3 samples follows a T^{-1} law, as shown in Fig. 4. This behavior is expected both in intrinsic semiconductors [13] and in mesoscopic systems [15]. The sign and the absolute value of the thermoelectric power depend on the details of energy dependence of the density of states (subject to broadening by imperfections) and on the nature of the scattering mechanism, both of which are beyond the scope of this Letter. The thermoelectric power of the Bi/SiO_2 nanocomposites decreases much more rapidly with temperature, indicating additional temperature-dependent mechanisms, such as two-carrier conduction. For comparison, we report in Fig. 3 the thermoelectric power of the 9 nm Zn/Al_2O_3 composites. It is almost an order of magnitude larger than that of bulk Zn[3]. However, as the thermoelectric power has a linear temperature dependence with a value $<20\ \mu V/K$, it remains consistent with metallic conduction in that system.

In summary, an experimental study of the resistance and the thermoelectric power of Bi/SiO_2 and Bi/Al_2O_3 nanocomposites is reported. The results show a very large increase in thermoelectric power, consistent with the theoretical predictions [4,6]. Also consistently with theory, the temperature dependence of both the resistance and the thermoelectric power of the nanocomposites are characteristic of a semiconductor, unlike the previously reported behavior of 200 nm diameter Bi nanowires, which are metallic. The present results constitute the first experimental confirmation of the concept of using one-dimensional quantum confinement to increase the thermoelectric power, and potentially the figure of merit, of thermoelectric materials. Values for the figure of merit of our samples could not be determined, as the filling fraction of Bi in the pores is unknown, and therefore so is the electrical resistivity. Zn-filled nanocomposites prepared for comparison using the same techniques and the same porous host materials remain metallic.

[1] M. J. Molina and F. S. Rowland, Nature (London) **249**, 810 (1974).
[2] D. A. Fisher, C. H. Hales, W. C. Wang, M. K. W. Ko, and N. D. Sze, Nature (London) **344**, 513 (1990).
[3] *Thermoelectric Handbook,* edited by D. M. Rowe (Chemical Rubber Company, Boca Raton, Florida, 1995), pp. 407 and 390.
[4] L. D. Hicks and M. S. Dresselhaus, Phys. Rev. B **47**, 12 727 (1993); **47**, 16 631 (1993).
[5] R. Venkatasubramanian, E. Silvola, T. Colpitts, and B. O'Quinn, Nature (London) **413**, 597 (2001).
[6] Y.-M. Lin, X. Sun, and M. S. Dresselhaus, Phys. Rev. B **62**, 4610 (2000).
[7] D. A. Glocker and M. J. Skove, Phys. Rev. B **15**, 608 (1977).
[8] Z. Zhang, X. Sun, M. S. Dresselhaus, J. Y. Ying, and J. P. Heremans, Appl. Phys. Lett. **73**, 1589 (1998).
[9] J. Heremans, C. M. Thrush, Y.-M. Lin, S. Cronin, Z. Zhang, M. S. Dresselhaus, and J. F. Mansfield, Phys. Rev. B **61**, 2921 (2000).
[10] J. Heremans and C. M. Thrush, Phys. Rev. B **59**, 12 579 (1999).
[11] S. Lowell and J. E. Shields, *Powder Surface Area and Porosity* (Chapman and Hall, London, 1984), 2nd ed., p. 54.
[12] R. R. Heikes and R. W. Ure, *Thermoelectricity: Science and Engineering* (Interscience Publishers, New York, 1961), p. 315.
[13] K. Seeger, *Semiconductor Physics* (Springer-Verlag, Berlin, 1985), 3rd ed., pp. 42 and 81–82.
[14] A. A. Abrikosov, *Fundamentals of the Theory of Metals* (North-Holland, Amsterdam, 1988), pp. 223–232.
[15] G. D. Guttman, E. Ben-Jacob, and D. J. Bergman, Phys. Rev. B **51**, 17 758 (1995).